Article

Not peer-reviewed version

Development of a Breathable Packaging Film for Fresh Products

Pedro V. Rodrigues , M. Cidália R. Castro * , Ana M. S. Soares , Liliana Melro , Ana V. Machado

Posted Date: 21 March 2024

doi: 10.20944/preprints202403.1224.v1

Keywords: polyethylene composites; microcrystalline cellulose; food packaging; surface functionalization

Article

Development of a Breathable Packaging Film for Fresh Products

Pedro V. Rodrigues, M. Cidália R. Castro *, Ana M. S. Soares, Liliana Melro and Ana V. Machado

Department of Polymer Engineering, Institute for Polymers and Composites (IPC), Campus de Azurém, University of Minho, 4804-533 Guimarães, Portugal; pedro.rodrigues@dep.uminho.pt; nita.soares@hotmail.com; liliana.melro@2c2t.uminho.pt; avm@dep.uminho.pt

* Correspondence: cidaliacastro@dep.uminho.pt;.

Abstract: In this study a material based on Polyethylene (PE) and Microcrystalline Cellulose (MC) was developed as a breathable packaging film. Surface functionalization of MC with 3 aminopropyltriethoxysilane (APTES) shows to be an efficient alternative to tailor their properties and increase opportunities for the application of MC on the reinforcement of polymers such polyethylene (PE). Functionalization of MC with mentioned silane derivative was achieved using a green method and later used on the development of composites with PE in three percentages (1, 3 and 5%). All the materials were prepared by melt blending and characterized, in terms of structural properties (ATR-FTIR and FTIR in transmittance, EDX, SEM), thermal properties (DSC and TGA), thermomechanical properties (DMA), contact angle measurements and permeability to oxygen and water vapor. The materials demonstrated to have potential to be used as breathable film packaging of fresh products.

Keywords: polyethylene composites; microcrystalline cellulose; food packaging; surface functionalization

1. Introduction

Depending on the type of food different barrier properties can be required. For example, a packaging film that enables retailers to market fresh foods with extended shelf-life without employing any major processing, preservatives or chemical additives would prevent a significant quantity of fresh products from spoiling [1,2].

Recently, due to the interest in environmentally friendly polymer composites, natural fibers have been used, enhancing mechanical properties and biodegradability of the polymer matrix. Cellulose, a natural fiber, is widely used as reinforcement for polymers due to its availability, great mechanical properties, low cost and biodegradability combined with unique characteristics such as low density, light weight, high specific area (that can interact more strongly with the matrix) and above all its, makes cellulose a potential eco-friendly additive [3]. Besides these properties cellulose could also modify the barrier properties of the polymer matrix. However, their hydrophilic character causes a poor compatibility with hydrophobic matrices, such polyethylene [4]. This problem can be easily solved since the presence of repetitive hydroxyl groups on the cellulose surface makes it suitable for several chemical modifications These changes are essential to increase the compatibility with a polymer matrix, which is an important requirement to achieve good mechanical properties [3,5–7]. PE filled with cellulose, can have a better compatibility through surface modification of cellulose by the addition of a coupling agent to the matrix. Intensive research on modification strategies of cellulose surface to improve the compatibilization degree between cellulose fibers and polymeric matrices has been performed [7–10]. Of all the coupling agents used, silane derivatives seem to be an excellent choice due to the diversity of functional groups and their commercial availability on a large scale. Moreover, the diversity of functional groups in silane coupling materials is a useful strategy that enhances the ability of covalent linkage between cellulose fibers and polymer matrices when two functional groups are presented. Usually, the general structure of silane coupling agents available are (RO)3-Si-R'-X, where alkoxy groups (RO) are capable to react with cellulose surface, rich in OH

 doi:10.20944/preprints202403.1224.v1

groups, intermediated by hydrolysis processes and the other group (R'-X) where R' is an alkyl chain and X is an organofunctional group that can be used to react with polymer matrix by covalent linkage [11,12]. From all variety of silane coupling agents, 3-aminopropyltriethoxysilane (APTES), the agent used in this study, is frequently used in silane modification due to its high reactivity, simplistic structure and low cost resulting in a cellulose-silica composite [13]. Nevertheless, the presence of an amine group on the APTES offers a good compatibilization by covalent linkage, via amine, with PE grafted with maleic anhydride. The modified PE (PE E226) used in this study is FUSABOND® E226 resin that is described by FDA as a material that can be used for packaging, transporting, or holding food, subject to the limitations and requirements therein.

Therefore, this work aims at developing a material that incorporates cellulose with good mechanical properties and barrier properties able to exchange gases for packaging application. First cellulose was modified with APTES and then the materials were obtained by reactive blending in a mixer. The structure, morphology and physical properties of the materials were characterized. Studies of surface hydrophobicity were also performed by contact angles measurement and permeability to water vapor and oxygen were carried out in to evaluate the barrier properties.

2. Materials and Methods

2.1. Materials

Polyethylene grafted with maleic anhydride (PE-g-MA, PE E226 FUSABOND®) was kindly provided by a Portuguese company. Microcrystalline cellulose (MC), *N,N*-dimethylacetamide (DMAc) were supplied from Acros Organics, while Lithium Chloride (LiCl), Ethanol and Ammonia solution 25 wt.% were purchased from Fisher Chemical. 3-aminopropyltriethoxysilane (APTES) 98% and Calcium Chloride anhydrous ($CaCl_2$) 93 % were acquired from Alfa Aesar. All materials were used without further purification.

2.2. Methods

2.2.1. Microcrystalline cellulose modification with 3-aminopropyltriethoxysilane Subsubsection

The modification of microcrystalline cellulose (MC) surface was carried out using a procedure already reported by Jia et al. [14]. First a solution with MC (1.4 g) and LiCl (1.5 g) in N,N-dimethylacetamide (20 mL) was left stirring at 90 ºC for 3 hours. Then, 5 mL of the previous MC solution was added to a mixture of ethanol (50 mL)/distilled water (10 mL) and promptly, 2 mL of ammonia solution (25 wt%) and 3-aminopropyltriethoxysilane (1 mL) were added at once to the colloidal solution, which was remained under strong stirring at room temperature for 24 h. The white precipitate was separated from the solution through centrifugation, washed with a mixture of water/ethanol and dried in the oven at 60 ºC under vacuum.

2.2.2. Microcomposites preparation

PE-*g*-MA and MC-APTES were dried overnight in a vacuum oven at 80ºC to prevent the hydrolysis of polymers during processing. Samples were prepared in batch mixer (Haake Rheomix Roller Roters R600, volume 69 cm^3), equipped with two rotors running in a counter-rotating way. Firstly, PE-*g*-MA was introduced inside the mixer and left around 2.5 min, then MC-APTES was added and a melt temperature of 140 ºC, 80 rpm and 7 min reaction time was used (Table 1). After, all materials were recovered in a metallic plate and left to cool under ambient conditions.

To achieve our purposes three materials were prepared adding 1, 3, and 5 wt.% of MC-APTES to the melt matrix. From the prepared materials, thin films were produced by compression moulding in a hot press at 140 ºC under a compressive force of 10 tons with an average thickness of 100 μm.

Table 1. Composition and processing conditions.

Composition code	Weight (%)		Processing conditions		
	PE-g-MA	MA-APTES	T_m (ºC)	Rotors speed (rpm)	t_{mixing} (min)

 doi:10.20944/preprints202403.1224.v1

PE-g-MA_1% MC-APTES	99	1	140	80	2.5 mixing + 7 reaction
PE-g-MA_3% MC-APTES	97	3			
PE-g-MA_5% MC-APTES	95	5			

2.3. Characterization

2.3.1. Fourier transformed infrared analysis (FTIR)

The Fourier Transformed Infrared (FTIR) analysis of the initial and modified materials was done on a Jasco 4100 FTIR spectrometer in ATR and transmittance mode for modified MC-APTES and for the prepared films (PE-*g*-MA_MC-APTES), respectively, in the range of 4500-400 cm^{-1} using 32 scans and a resolution of 8 cm^{-1}.

2.3.2. Themal analysis

Thermogravimetric analysis (TGA) was performed using a TA Q500 thermogravimetric analyzer (TA Instruments, New Castle, DE, USA). The samples (approximately 15 mg) were placed in a platinum crucible and heated from 40 °C to 600 °C at a heating rate of 10 °C/min under a nitrogen flow (60 mL/min). The initial decomposition temperature (Tonset), the derivative maximum decomposing rate temperature (Tmax), and the residual weight were determined.

Differential scanning calorimetry (DSC) analysis was accomplished in a Netzsch 200 Maya (Netzsch, Selb, Germany), approximately 4 mg of each sample was cut and placed in an aluminium pan. A heating/cooling ramp was run at 10 °C/min, between 25 °C and 200 °C under nitrogen, for each sample.

The degree of crystallinity χ_c was calculated according to equation (1), as described in [15]:

$$\chi_c(\%) = \frac{\Delta H_m}{W_f . \Delta H_m^0} \times 100\% \quad (1)$$

where W_f is the PE-*g*-MA weight fraction, ΔH_m^0 is the theoretical melting enthalpy of 100% crystalline PE (293 J/g) [16] and ΔH_m the melting enthalpy of our sample.

2.3.3. Scanning electron spectroscopy analysis (SEM)

The morphology of the surface and cross-section of the samples was analysed using a Leica Cambridge S360 scanning electron microscope. The samples were previously placed in liquid nitrogen and then fractured, followed by a gold thin coating. Energy-Dispersive X-ray analysis (EDX) was performed to confirm the presence of Si.

2.3.4. Dynamic mechanical analysis (DMA)

Dynamic mechanical analysis measurements were made on rectangular films with same dimensions (2×0.5cm×0.5µm) using a Triton Technology DMA. Samples were evaluated using a dynamic temperature sweep to measure the storage modulus and loss moduli (E′ and E′′) at a constant frequency (1 Hz), constant force (1N) and a constant heating rate of 3 °C/min in oscillatory mode in a range of temperatures between 30 ºC and 110 ºC. The measurements were made three times for each composite.

2.3.5. Contact angle measurements (CA)

CA measurements (Contact Angle System OCA 20 Dataphysics, Germany) using distilled water (volume: 3 µL; rate: 2 µL/s) that was dropped on the film surface with a precision syringe using the sessile drop method. The initial image of the drop (taken by 0 seconds) was recorded with a video camera. At least 20 measurements per film were carried out and the mean value was taken. The contact angles were calculated by Laplace-Young Fitting method.

2.3.6. Water Vapor Permeability (WVP)

The water vapor transmission rate (WVTR) of films was determined by the ASTM method E96 [17]. The desiccant method was used to determine the value of water vapor transmission. The films

 doi:10.20944/preprints202403.1224.v1

were placed in circular metal test dishes with a surface diameter of 69.50 mm and filled with ~ 25 g of CaCl2 anhydrous, previously dried in a vacuum oven at 150 ºC overnight. Then were sealed with parafilm to ensure that humidity migration occurred exclusively through the film. Next, the test cups were placed in a desiccator and kept at room temperature and 94.26±4.33% Relative Humidity (RH) in triplicate and weighed daily for one month. The measured WVTR of the films was calculated using Equation (2):

$$\text{WVTR(g water/(m}^2\text{. hour))} = \frac{G}{t \times A} \quad (2)$$

where G/t (g water/hour) is the slope (weight *versus* time plot), and A is effective film area (m^2). WVTR was calculated using three replications and expressed in $g.h^{-1}m^{-2}$.

3. Results and Discussion

The reaction between MC and APTES was performed in solvent, LiCl and DMAc as a mixture of solvent is an important factor once the formed complex ([(DMAc)$_2$–Li]Cl) penetrate into the cellulose structure, acting as spacers in the MC packing chains, which facilitates the chemical modification [18]. Therefore, the reaction with silane coupling agent, APTES, occurred successfully and could be confirmed by complementary analysis of ATR-FTIR Figure 1 and EDX Figure 2. The modification of MC with APTES was detected by the appearance of an additional peak at 1562 cm^{-1}, corresponding to the bending vibration of -NH_2 groups, indicating that they were successfully introduced onto the MC surface. The adsorption peak of Si–O–Si vibration, characteristic of the self-condensation occurred between the silane reaction with cellulose hydroxyl groups, at around 1000 - 1100 cm^{-1} is overlapped with the C-O-C vibration bands of cellulose around 950-1200 cm^{-1}. Moreover, the band corresponding to the Si-O-Cellulose, around 1150 cm^{-1}, could not be observed due to the presence of the large and intense C-O-C vibration bands of cellulose [13,19,20].

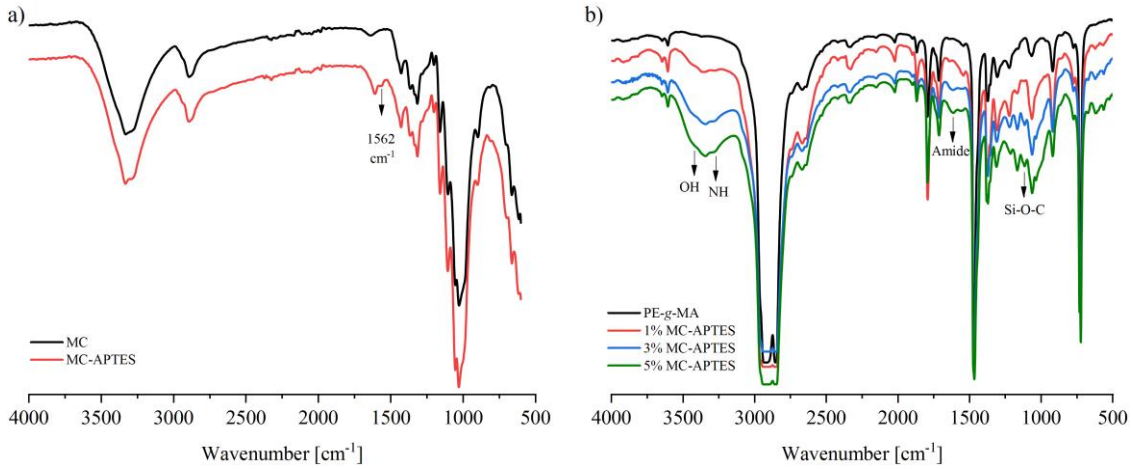

Figure 1. a) ATR-FTIR spectra of MC, MC-APTES; b) Transmitance-FTIR spectra of PE-*g*-MA-MC-APTES films.

 doi:10.20944/preprints202403.1224.v1

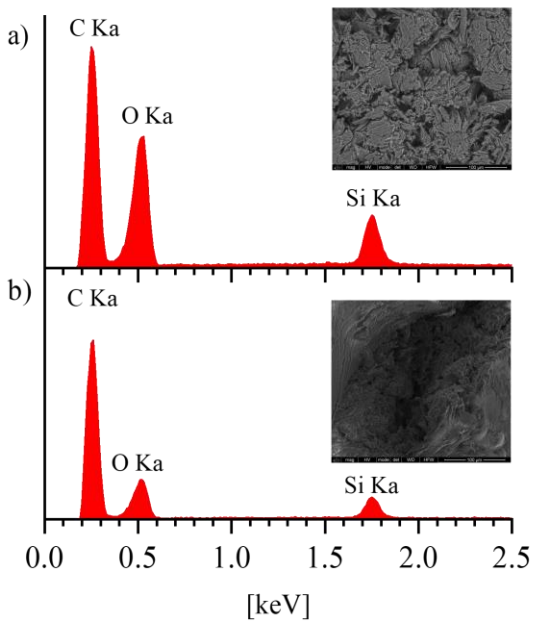

Figure 2. EDX spectra of MC-APTES (a)) and PE-*g*-MA reacted with 5% (b)) of MC_APTES.

After the incorporation of modified cellulose in the polymer, a reaction occurs trough amide linkage between the amine group of cellulose-silane and maleic anhydride grafted onto PE, as illustrated on Scheme 1.

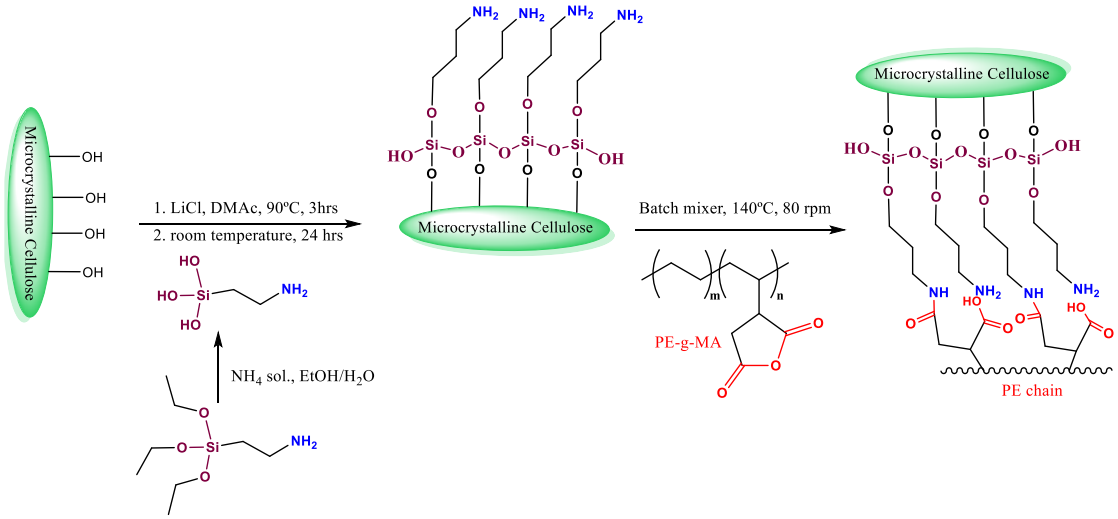

Scheme 1. Reaction scheme of PE-g-MA and MC-APTES.

According to ATR-FTIR results (Figure 2a) both samples exhibited absorption peaks that are characteristic of cellulose, namely the peaks at 3318, 2859, 1428, 1315 and 1025 cm^{-1}, which are associated to the vibration of –OH, C–H, –CH_2 and C–O, respectively.

Films of the prepared materials and PE-g-MA were analyzed by FTIR in transmittance mode and are depicted in Figure 1b. The covalent linkage between PE-g-MA and modified cellulose was confirmed by the disappearance of the bending vibration -NH2 at 1562 cm^{-1}, which demonstrate that the amino groups on the cellulose surfaces were converted to –NH–band at 3320 cm^{-1} and amide band around 1613 cm^{-1}. Moreover, the bands intensity increases with increasing content of modified cellulose, and there is also a growth of the broad band related to the -OH groups of cellulose and to the consequent succinic ring opening.

The presence of silicon (Si) and oxygen (O) in the polymer matrix assessed by EDX are present in Figure 2. Figure 2a corresponds to the modified MC, where the O and Si peaks have a significant

 doi:10.20944/preprints202403.1224.v1

intensity. As expected, a lower intensity can be observed in Figure 2b, which corresponds to the samples containing 5 wt.% of MC-APTES, respectively. Even though the peaks intensity increased with the amount of MC-APTES incorporated, they are almost undetected for the samples containing 1 wt.%. This can be due to the heterogeneous dispersion of the MC-APTES in the matrix that made the evaluation more complicated since only points are selected in this kind of analysis.

SEM micrographs of PE-*g*-MA and PE-*g*-MA containing 5 wt.% MC-APTES are represented in Figure 3. Since the micrographs of the materials with 1 and 3 wt.% of MC-APTES are very similar to the one with 5% MC-APTES, only the latter is presented. The surface and cross-section of PE-*g*-MA film, Figure 3a, revealed smooth and homogeneous surfaces, whereas the film that incorporates MC-APTES exhibits a rough surface, Figure 3b. Moreover, in the cross-section of the same samples Figure 3b it is possible to noticed that MC-APTES located along the sample and at the surface. As expected from the chemical results a good adhesion between the modified MC and polymer was achieved.

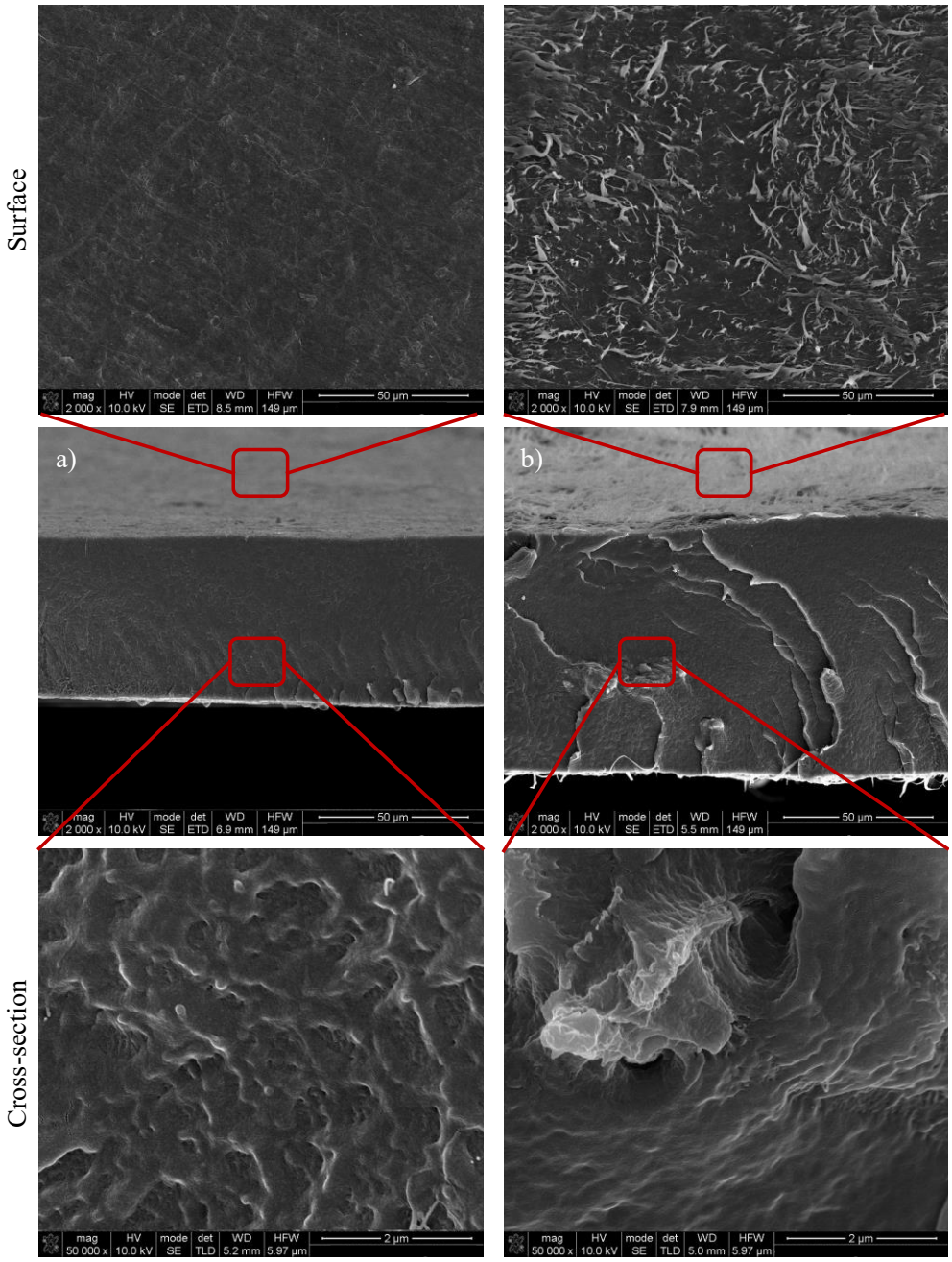

Figure 3. Sample surface and cross-section SEM micrographs of a) PE-g-MA and b) PE-g-MA+5%MC-APTES.

 doi:10.20944/preprints202403.1224.v1

The effect of MC functionalization with APTES on its thermal properties and incorporation in the PE matrix was evaluated (Figures 4 and 5, respectively). Figure 4a depicts the thermal decomposition of MC and modified MC, where it is possible to observe an initial weight loss (~5%) around T = 80 ºC, for MC, probably due to the vaporization of adsorbed water. The modification of MC surface with APTES increases both initial thermal degradation and temperature at the maximum degradation rate, with a difference around 10º C between MC (250.6 ºC) and MC-APTES (361.2 ºC), as it can be seen in Figure 4b. This increase in the thermal stability of MC-APTES may be assigned to the good interaction amongst the APTES and MC and their consequent crosslinking reactions occurred during the functionalization. Moreover, the results also demonstrate that, for T= 500 ºC, MC-APTES have a higher residual mass value than unmodified MC, 26.9 and 14.6 %, respectively. This result can be associated the presence of siloxy moieties on MC-APTES product that remain as a residue. These results are in agreement with the results reported by H. Khanjanzadeh *et* al. [13].

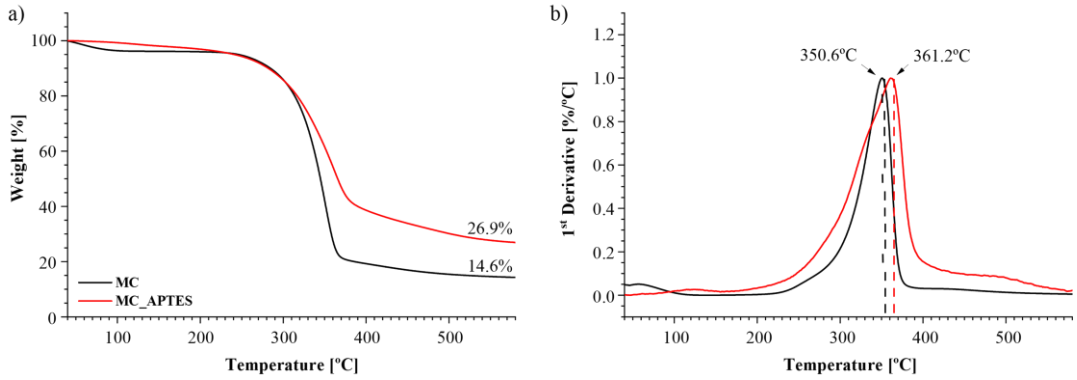

Figure 4. TGA curve weight loss (a)) and 1st derivative (b)) of unmodified MC and modified MC.

TGA results of the prepared materials, Figure 5, reveal that despite an earlier decomposition temperature between 320-343 ºC can be noticed, the thermal stability is slightly enhanced since the degradation peak of PE matrix shifts to higher temperatures. Whereas the curve for PE-*g*-MA presented only one thermal degradation stage with mass loss of almost 100 %, the curve of the other samples displays two thermal degradation stages. The first degradation peak related to cellulose degradation (320-343 ºC), and as expected, increasing the MC-APTES amount increases the weight loss (around 4.5%) and a decrease on the decomposition temperature value, Figure 5b. The same occurs for the degradation peak of PE (478-479 ºC), the sample with 1%MC-APTES seems to be the most thermal stable composite when compared with the other composites. This is in accordance with literature, Ch.V.Alexanyan *et al* reported a study where it's possible to verify that the presence of cellulosic materials translates in a slight increase in the degradation temperature. Moreover, the charcoal, resulted from cellulose degradation, contribute to the hydrogenation of the unsaturated products and, consequently, the hydrogenated products develop at higher temperature [21].

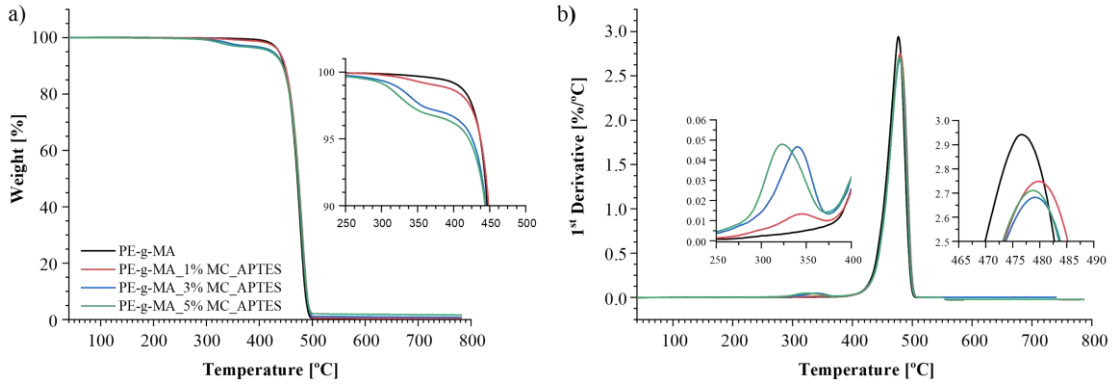

Figure 5. TGA curve weight loss (a)) and 1st derivative (b)) of PE-*g*-MA and PE-*g*-MA-MC-APTES composites.

 doi:10.20944/preprints202403.1224.v1

The DSC experimental curves of PE-*g*-MA_MC-APTES composites obtained from the first heating and cooling cycle are displayed at Figure 6 and Table 2.

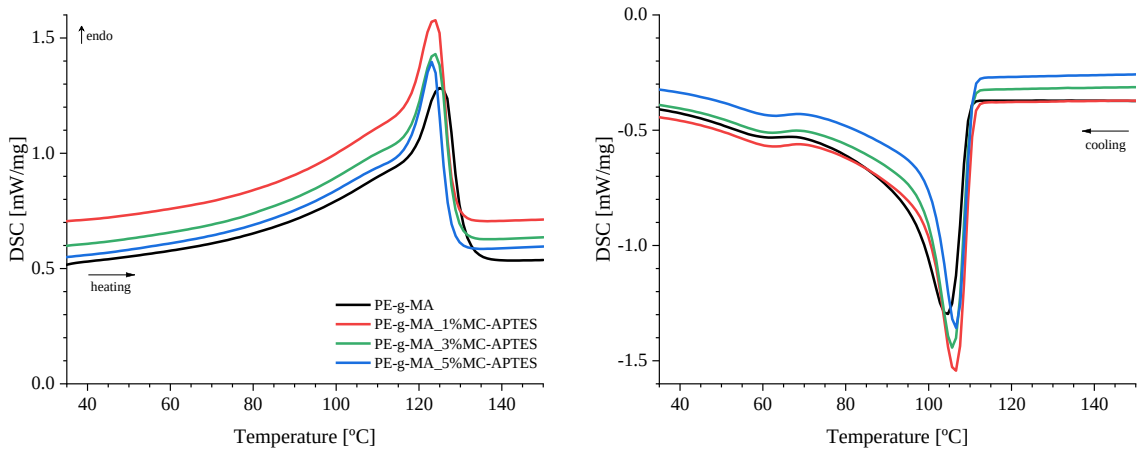

Figure 6. Thermal behavior of PE-g-MA and prepared samples.

Table 2. DSC results for PE-*g*-MA composites: PE-*g*-MA, PE-*g*-MA_1%MC-APTES, PE-*g*-MA_3%MC-APTES, PE-*g*-MA_5%MC-APTES.

Sample	ΔHm [J/g]	Xc [%]	Tm [ºC]	Tc [ºC]
PE-g-MA	123.9	42.3	125	105
1% MC-APTES	126.8	43.7	124	107
3% MC-APTES	120.3	42.3	124	106
5% MC-APTES	111.8	40.2	123	107

Crystalline polymers are characterized by a melting transition at a certain temperature, the melting temperature (T_m) and enthalpy (ΔH) for melting. The crystallinity of the PE was in the range of 40–44% for all studied composites, where the crystallinity of neat PE-*g*-MA is 42.9%. The presence of MC slightly shifts the melting point of PE-g-MA for lower temperatures, narrowing the peak. This could be evidence that the presence of cellulose in the matrix induces less stable crystals. On the other hand, cellulose can act as a nucleating agent during the cooling cycle, whereas the crystallization peak starts at higher temperatures. Although this results, no significant changes on crystallinity are detected, which cannot be related to the following characterization of the film properties.

Dynamic mechanical results of all materials exhibited an increase in Storage Modulus as the amount of modified MC content in the polymer increases. This is associated the reinforcement effect of the MC. Moreover, the shift of Tan Delta to lower temperatures, this in agreement with E' enhancement. As the shift to lower temperatures, indicates a better compatibilization between modified MC and the polymer matrix.

 doi:10.20944/preprints202403.1224.v1

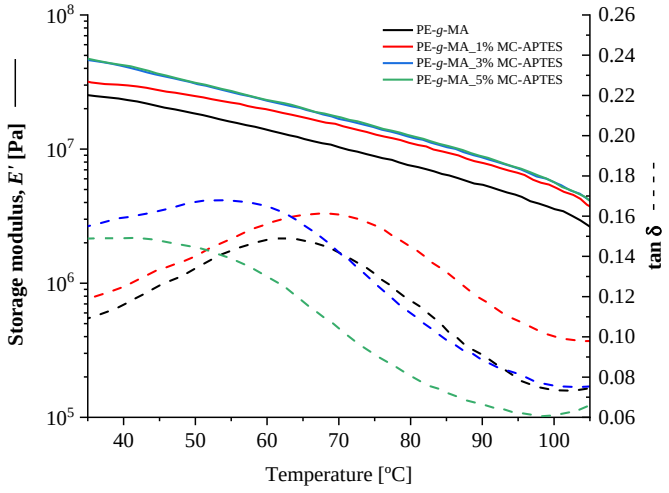

Figure 7. Storage modulus (solid) and Tan δ (dash) obtained by DMA for neat PE-*g*-MA and PE_MC-APTES composites.

Polyethylene is known as a hydrophobic polymer, meaning that wetting ability is very low, which can be a disadvantage in food applications. Therefore the incorporation of a more hydrophilic materials, such as, cellulose and/or cellulose-silane composites, could increase the wettability capacity [22].

Distilled water (volume: 3 μL; rate: 2 μL/s) was dropped on the film surface with a precision syringe using the sessile drop method. The image of the initial drop (taken at 0 seconds) was recorded with a video camera, the contact angles along with the drop image is depicted in Figure 8. As expected, the increase of MC-APTES content on PE matrix increases the surface wettability and decreases the contact angle. The CA of PE-*g*-MA is around 90º, due to the hydrophobic nature of PE, while for the materials with 1, 3 and 5% of MC-APTES, the CA are approximately 83º, 81º and 79º, respectively. This means that the surface of the film became more hydrophilic with increasing cellulose content, as already reported in literature [22–24]. Thus, these results are in agreement with the obtained surface SEM image, Figure 3b, where is possible to observe the presence of modified cellulose on film surface. Thus, it is visible the effect of cellulose on the hydrophilic character of the prepared materials, since the hydroxyl groups present in cellulose are able to form strong hydrogen bonds with the water molecule. Therefore, it´s possible to change the hydrophilicity/hydrophobicity on the material changing the MC content.

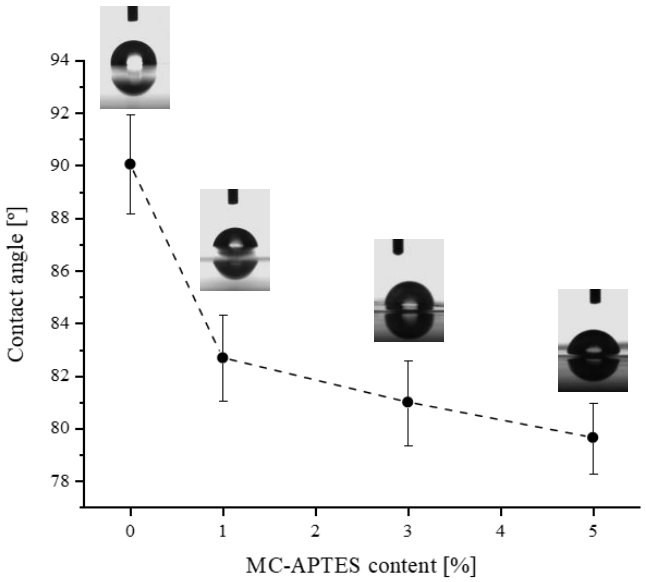

Figure 8. Contact angle of PE-*g*-MA and prepared samples.

 doi:10.20944/preprints202403.1224.v1

Water vapor barrier property is vital for packaging, which can prevent or allow the transmission of this gas from the atmosphere to the food. Therefore, is crucial to control the transmission of gases/moisture from the environment to the food to extend the shelf life and quality of food [25]. The incorporation of a more hydrophilic materials, as cellulosic derivatives, can change barrier properties to gases. Although cellulose displays an effective barrier to gases, when it is in a humid environment, cellulose swells, to overcome this drawback and to afford a hydrophobic character, chemical functionalization have been carried out on the cellulose structure [26]. Despite the silanization of the cellulose surface, a smaller number of hydroxyl groups still available to linkage water molecules promoting a path for water vapor.

The WVTR characterizes the capability of moisture to penetrate and pass through the film and it was assessed to understand the effect of MC-APTES content on films water vapor transmission, Figure 9. The results of WVTR demonstrate that the addition of modified cellulose in the PE matrix increased the WVTR of the films from 0.13± 0.030 $g.h^{-1}m^{-2}$ (PE-*g*-MA) to 0.29±0.026; 0.37±0.038 and 0.69±0.015 $g.h^{-1}m^{-2}$ of the films with 1, 3 and 5%MC-APTES, respectively. The presence of modified MC results in a lower barrier to water molecules when compared PE-g-MA, and an increase from 3 to 5% MC-APTES raises the WVTR almost twice, 0.37 and 0.69 $g.h^{-1}.m^{2}$, respectively. This agrees with literature results, where it is reported that cellulose increases barrier properties due to their solid web-like architecture.

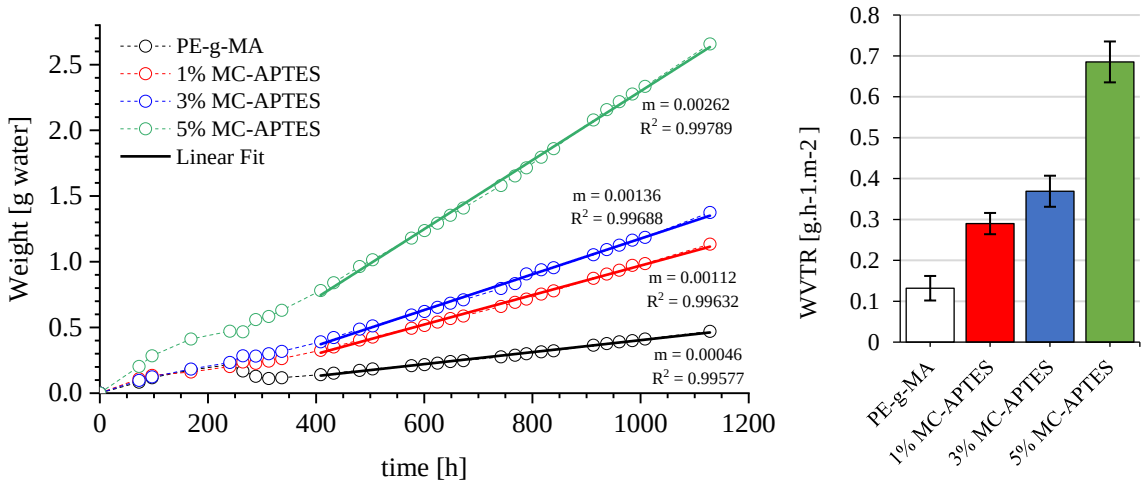

Figure 9. Water vapor permeability along time (left) and WVTR (right) of all materials films.

4. Conclusions

An environmental-friendly and simple modification of MC surface with silane derivatives, as showed in FTIR analysis, and posterior melt blending whit PE-g-MA allowed to develop a material with good adhesion between the two phases. SEM studies reveals strong interactions between the amino-silane groups attached to the cellulose and the MA grafted in PE matrix. Consequently, the mechanical properties improved when compared to the polymer matrix. Moreover, the introduction of modified cellulose in PE matrix results in an increase of thermal stability, shifting the degradation peak of PE matrix to higher temperatures.

The hydrophilicity and water vapor transmission of produced films can be controlled depending on MC-APTES contents, and increasing the MC-APTES content, increase the wettability of the film and consequently decrease the CA. For example, the CA of PE-g-MA_5%MC-APTES composite is significantly lower than for neat PE-*g*-MA, ~79º and ~90º, respectively, which means more hydrophilic film. Similarly, increasing the MC-APTES content results in higher WVTR comparatively to neat PE-*g*-MA.

Therefore, the strategy used allows us to prepare packaging films with good mechanical properties and gases transmission for fresh products.

Author Contributions: Conceptualization, M.C.R.C., A.M.S.S. and A.V.M.; methodology, P.V.R., M.C.R.C., A.M.S.S. and A.V.M.; software, P.V.R. and L.M..; validation, A.M.S.S. and A.V.M.; formal analysis, P.V.R., M.C.R.C., A.M.S.S. and A.V.M.; investigation, M.C.R.C., A.M.S.S. and L.M.; resources, A.V.M.; data curation, P.V.R., M.C.R.C., A.M.S.S. and A.V.M.; writing—original draft preparation, A.M.S.S. and L.M; writing—review and editing, P.R.V., M.C.R.C. and A.V.M.; visualization, A.V.M.; supervision, A.V.M.; project administration, A.V.M.; funding acquisition, A.V.M. All authors have read and agreed to the published version of the manuscript.

Funding: This research was funded within the scope of the project TSSiPRO - technologies for sustainable and smart innovative products - NORTE- 01-0145-FEDER-000015. The authors also acknowledge the financial support by Portugal 2020, and Fundo Social Europeu (FSE) through Programa Operacional Regional do NORTE (NORTE-08-5369--FSE-000034), developed under the program "IMPULSE - Polímeros e Compósitos: Drivers da inovação tecnológica e da competitividade industrial".

Data Availability Statement: The raw/processed data required to reproduce these findings cannot be shared at this time as the data also forms part of an ongoing study.

Acknowledgments: No information.

Conflicts of Interest: "The authors declare no conflicts of interest."

References

1. K. Czerwiński, T. Rydzkowski, J. Wróblewska-Krepsztul, and V. K. Thakur, "Towards Impact of Modified Atmosphere Packaging (MAP) on Shelf-Life of Polymer-Film-Packed Food Products: Challenges and Sustainable Developments," Coatings, vol. 11, no. 12, p. 1504, 2021. [Online]. Available: https://www.mdpi.com/2079-6412/11/12/1504.
2. O. J. Caleb, P. V. Mahajan, F. A.-J. Al-Said, and U. L. Opara, "Modified Atmosphere Packaging Technology of Fresh and Fresh-cut Produce and the Microbial Consequences—A Review," Food and Bioprocess Technology, vol. 6, no. 2, pp. 303-329, 2013/02/01 2013, doi: 10.1007/s11947-012-0932-4.
3. C. Miao and W. Hamad, "Cellulose reinforced polymer composites and nanocomposites: A critical review," Cellulose, vol. 20, 10/01 2013, doi: 10.1007/s10570-013-0007-3.
4. H. Yano, H. Omura, Y. Honma, H. Okumura, H. Sano, and F. Nakatsubo, "Designing cellulose nanofiber surface for high density polyethylene reinforcement," Cellulose, vol. 25, 06/01 2018, doi: 10.1007/s10570-018-1787-2.
5. M. Zimniewska, M. Wladyka-Przybylak, and J. Mankowski, "Cellulose Fibers: Bio- and Nano-Polymer Composites," 2011, pp. 97-119.
6. D. K. Rajak, D. D. Pagar, P. L. Menezes, and E. Linul, "Fiber-reinforced polymer composites: Manufacturing, properties, and applications," Polymers, vol. 11, no. 10, p. 1667, 2019.
7. H. Mohit and V. Arul Mozhi Selvan, "A comprehensive review on surface modification, structure interface and bonding mechanism of plant cellulose fiber reinforced polymer based composites," Composite Interfaces, vol. 25, no. 5-7, pp. 629-667, 2018/07/03 2018, doi: 10.1080/09276440.2018.1444832.
8. K. Missoum, N. Belgacem, and J. Bras, "Nanofibrillated Cellulose Surface Modification: A Review," Materials, vol. 6, pp. 1745-1766, 05/01 2013, doi: 10.3390/ma6051745.
9. H. Abushammala and J. Mao, "A Review of the Surface Modification of Cellulose and Nanocellulose Using Aliphatic and Aromatic Mono- and Di-Isocyanates," (in eng), Molecules (Basel, Switzerland), vol. 24, no. 15, Jul 31 2019, doi: 10.3390/molecules24152782.
10. M. Tavakolian, S. Jafari, and T. van de Ven, "A Review on Surface-Functionalized Cellulosic Nanostructures as Biocompatible Antibacterial Materials," Nano-Micro Letters, vol. 12, 12/01 2020, doi: 10.1007/s40820-020-0408-4.
11. Y. Xie, C. A. S. Hill, Z. Xiao, H. Militz, and C. Mai, "Silane coupling agents used for natural fiber/polymer composites: A review," Composites Part A: Applied Science and Manufacturing, vol. 41, no. 7, pp. 806-819, 2010/07/01/ 2010, doi: https://doi.org/10.1016/j.compositesa.2010.03.005.
12. C. K. Jayasuriya, "Interfacial Bonding in Polymer–Ceramic Nanocomposites☆," in Reference Module in Materials Science and Materials Engineering: Elsevier, 2017.
13. H. Khanjanzadeh et al., "Surface chemical functionalization of cellulose nanocrystals by 3-aminopropyltriethoxysilane," International Journal of Biological Macromolecules, vol. 106, pp. 1288-1296, 2018/01/01/ 2018, doi: https://doi.org/10.1016/j.ijbiomac.2017.08.136.
14. N. Jia, S.-M. Li, M.-G. Ma, J. Zhu, and R.-C. Sun, "Synthesis and characterization of cellulose-silica composite fiber in ethanol/water mixed solvents," Bioresources, vol. 6, 02/23 2011, doi: 10.15376/biores.6.2.1186-1195.
15. E. Tarani, I. Arvanitidis, D. Christofilos, D. N. Bikiaris, K. Chrissafis, and G. Vourlias, "Calculation of the degree of crystallinity of HDPE/GNPs nanocomposites by using various experimental techniques: a

comparative study," Journal of Materials Science, vol. 58, no. 4, pp. 1621-1639, 2023/01/01 2023, doi: 10.1007/s10853-022-08125-4.
16. F. Mirabella and A. Bafna, "Determination of the crystallinity of polyethylene/?-olefin copolymers by thermal analysis: Relationship of the heat of fusion of 100% polyethylene crystal and the density," Journal of Polymer Science Part B: Polymer Physics, vol. 40, pp. 1637-1643, 08/15 2002, doi: 10.1002/polb.10228.
17. ASTM E96/E96M-16-Standard Test Methods for Water Vapor Transmission of Materials, 2015.
18. N. Kotov, V. Raus, and J. Dybal, "Intermolecular Interactions in N,N-Dimethylacetamide without and with LiCl Studied by Infrared Spectroscopy and Quantum Chemical Model Calculations," The Journal of Physical Chemistry B, vol. 122, no. 38, pp. 8921-8930, 2018/09/27 2018, doi: 10.1021/acs.jpcb.8b05569.
19. Y. Liu et al., "Characterization of Silane Treated and Untreated Natural Cellulosic Fibre from Corn Stalk Waste as Potential Reinforcement in Polymer Composites," Carbohydrate Polymers, vol. 218, pp. 179-187, 08/15 2019, doi: 10.1016/j.carbpol.2019.04.088.
20. M. Bengtsson and K. Oksman, "The use of silane technology in crosslinking polyethylene/wood flour composites," Composites Part A: Applied Science and Manufacturing, vol. 37, no. 5, pp. 752-765, 2006/05/01/ 2006, doi: https://doi.org/10.1016/j.compositesa.2005.06.014.
21. S. M. Lomakin, S. Z. Rogovina, A. V. Grachev, E. V. Prut, and C. V. Alexanyan, "Thermal degradation of biodegradable blends of polyethylene with cellulose and ethylcellulose," Thermochimica Acta, vol. 521, no. 1, pp. 66-73, 2011/07/10/ 2011, doi: https://doi.org/10.1016/j.tca.2011.04.005.
22. M. A. Hubbe et al., "Nanocellulose in Thin Films, Coatings, and Plies for Packaging Applications: A Review," 2017, Barrier properties; Water vapor transmission; Food shelf life; Oxygen transmission; Packages; Cellulose nanomaterials vol. 12, no. 1, p. 91, 2017-02-01 2017. [Online]. Available: https://ojs.cnr.ncsu.edu/index.php/BioRes/article/view/BioRes_12_1_2143_Hubbe_Review_Nanocellulose_Thin_Films_Coatings_Plies/5093.
23. X. Dang, X. Cao, L. Ke, Y. Ma, J. An, and F. Wang, "Combination of cellulose nanofibers and chain-end-functionalized polyethylene and their applications in nanocomposites," Journal of Applied Polymer Science, vol. 134, no. 42, p. 45387, 2017, doi: https://doi.org/10.1002/app.45387.
24. O. G. d. S. Junior, R. P. de Melo, R. d. B. C. Sales, E. Ayres, and P. S. d. O. Patricio, "Processing and characterization of polyethylene/starch/curauá composites: Potential for application as thermal insulated coating," Journal of Building Engineering, vol. 11, pp. 178-186, 2017/05/01/ 2017, doi: https://doi.org/10.1016/j.jobe.2017.04.016.
25. V. Siracusa, "Food Packaging Permeability Behaviour: A Report," International Journal of Polymer Science, vol. 2012, p. 302029, 2012/05/07 2012, doi: 10.1155/2012/302029.
26. G. Fotie, S. Limbo, and L. Piergiovanni, "Manufacturing of Food Packaging Based on Nanocellulose: Current Advances and Challenges," Nanomaterials, vol. 10, p. 1726, 08/31 2020, doi: 10.3390/nano10091726.